Contract No:

This document was prepared in conjunction with work accomplished under Contract No. DE-AC09-08SR22470 with the U.S. Department of Energy (DOE) Office of Environmental Management (EM).

Disclaimer:

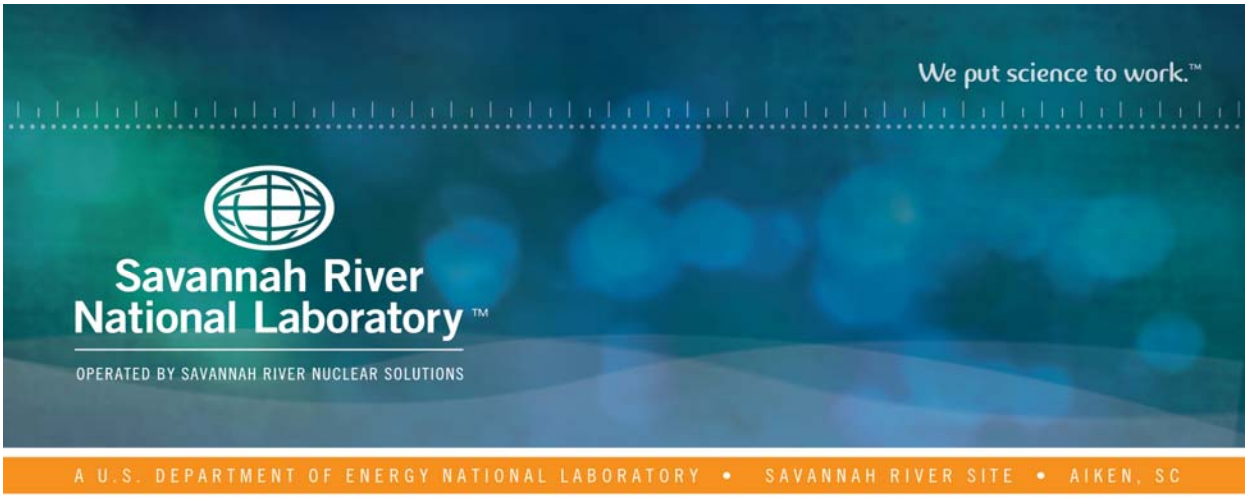

Evaluation of Radiation Proofing Polyethylene: Use of Oxygen Scavenging Additives

Leroy Magwood

Thanh-Tam Truong

Aaron L. Washington, II

October 2017

SRNL-STI-2017-00613, Revision 0

DISCLAIMER

Printed in the United States of America

Prepared for
U.S. Department of Energy

SRNL-STI-2017-00613
Revision 0

Keywords: *Oxygen Reduction, Polyethylene Lifetime, Alpha Degradation, Radiation Proof, Radiation Bag, Radiation Containment*

Retention: *Permanent*

Evaluation of Radiation Proofing Polyethylene: Use of Oxygen Scavenging Additives

Leroy Magwood
Thanh-Tam Truong
Aaron Washington, II

October 2017

Prepared for the U.S. Department of Energy under contract number DE-AC09-08SR22470.

Savannah River National Laboratory™
OPERATED BY SAVANNAH RIVER NUCLEAR SOLUTIONS

REVIEWS AND APPROVALS

AUTHORS:

Leroy Magwood, Chemical Processing Technology Date

Thanh-Tam Truong, Materials Science and Technology Date

Aaron Washington, II, Chemical Processing Technology Date

TECHNICAL REVIEW:

Jonathan Christian, Chemical Processing Technology, Reviewed per E7 2.60 Date

APPROVAL:

Boyd Wiedenman, Manager Date
Chemical Processing Technology

David Dooley, Director, Environmental & Chemical Process Technology Research Programs Date

Michael Serrato, Environmental Restoration Technologies Date

PREFACE OR ACKNOWLEDGEMENTS

The authors wish to thank Payton Folk for her tireless efforts synthesizing doped-zinc nanoparticles during her summer internship. We also thank to Josef Velten for his assistance with SEM scans.

EXECUTIVE SUMMARY

The degradation of polyethylene (PE) from radiation sources with both thermal and nuclear interactions show sensitivities towards oxygen and air. Characterization of the sensitivities in both inert and oxygenated atmospheres can be characterized by thermogravimetric analysis (TGA). Under argon, the thermal degradation of PE follows a random scission pathway that has activation energy of ~229 kJ mol^{-1}. The activation energy of PE is reduced by ~30% when 1% air is added to the inert argon atmosphere, illustrating the impact of oxygen on the degradation of PE. This effort seeks to diminish degradation of PE waste containment bags and extend their lifetime, thereby, reducing the cost and worker exposure risk. The project evaluated the use of oxygen scavenger nanoparticles to mitigate the deteriorating effects of oxygen on polymer physical properties and reduce polymer degradation. The thermal degradation of PE composites with various additives were tested and two additives showed promising results approaching the activation energy of pristine PE in an inert atmosphere. This activity was sponsored by the EM Office of Technology Development through SRNL's Technical Task Plan SR091701.

TABLE OF CONTENTS

LIST OF TABLES

LIST OF FIGURES

LIST OF ABBREVIATIONS

Ba	Barium
C_{60}	Buckminster fullerene
CO_2	Carbon Dioxide
D&D	Deactivation and Decommissioning
EPR	ethylene-propylene rubber
FTIR	Fourier Transform Infrared Spectroscopy
$LiBH_4$	lithium borohydride
N_2	Nitrogen
NP(s)	Nanoparticle(s)
O_2	Oxygen
PE	Polyethylene
PVA	Polyvinyl Alcohol
SEM	Scanning Electron Microscopy
T_g	Glass Transition Temperature
T_m	Maximum Temperature from DTA Curve
TGA	Thermogravimetric Analyzer
XLPE	crosslinked polyethylene
Zn	Zinc
ZnO	Zinc Oxide

1.0 Introduction

Polymers are ubiquitously used in nuclear facilities with applications; as seals, piping/tubing [1], hoses, electrical and thermal insulation, pump/valve components, lubricants [2] and personal protective equipment. Deactivation and decommissioning (D&D) activities for a nuclear facility can range from collection of small parts and instruments to active ores that emit radiological signals and involve both handling and packaging of collected items into containment barriers. PE was chosen as a suitable containment/barrier layer because of its normally inert nature and the ability to avoid leaks that could result in unwanted contamination and exposure to workers; more specifically alpha radiation. However, PE like other polymers degrades in radiological environments due to both radiolytic and thermal interactions under sustained exposure and must be periodically replaced.

Christian et al. [3] reported the development of radiation resistant C_{60}-doped polyvinyl alcohol (PVA) films. These films could withstand approximately seven times more α radiation than undoped PVA or PE films when tested using an alpha particle accelerator. However, it is important to note that since these films were evaluated in a vacuum sealed chamber within the alpha particle accelerator, oxygen, which is essential to the oxidative degradation reaction was not present. Singh [4] studied the impact of the gamma irradiation of polyethylene in both air and inert atmosphere. Singh noted that crosslinking was the dominant process when PE is irradiated in an inert atmosphere. However, when PE is irradiated in air, oxidative degradation becomes the dominant process; this is particularly true at a low-dose-rate of gamma irradiation. The impact of gamma on the physical properties of PE has also been studied. Gillen et al. [5] determined that PE aged at a temperature of 80°C in the presence of air experiences a 5% loss in the elongation over a 100-day period. PE exposed to a 5 krad/hr gamma dose, experiences an increased loss of elongation over thermal aging alone resulting in a total loss of ~25% over the same 100-day period. The combination of thermal aging at 80°C and exposure of PE to gamma at 5 krad/hr in an air atmosphere lead to complete material failure within 100 days. However, PE aged at 80°C and gamma exposure at 5 krad/hr in a N_2 atmosphere does not experience a loss in the elongation, suggesting that although crosslinking occurs in the N_2, its impact on physical properties such as elongation is minimal.

Reed et al. [6] evaluated the net gas generated from polyethylene and polyvinyl chloride during irradiation from an alpha source under varying temperatures and levels of atmospheric oxygen. From their studies, it was noted that in the absence of oxygen and at low temperatures the degradation of PE is slow. However, irradiating PE at oxygen levels typically found in the atmosphere (~21% O_2) creates a significant evolution of gases from the polymer including molecular hydrogen (H_2) and carbon dioxide (CO_2), suggesting that molecular oxygen is a key driver in the alpha degradation process.

A similar effect of oxygen is noted during the thermo-oxidative degradation of PE and other polymers using a thermogravimetric analyzer (TGA) [7 – 10]. Many authors have evaluated the use of antioxidants, that are effective in the thermal degradation, for their ability to mitigate radiation induced oxidation. Seguchi et al. [10] showed that the activation energy of a polymer changed during thermal oxidative degradation within the range of 100 – 120°C for both ethylene-propylene rubber (EPR) and crosslinked polyethylene (XLPE). This is attributed to the decreased number of antioxidants in the polymer due to evaporation. Although the organic antioxidants that are used in both EPR and XLPE significantly reduced the extent of thermal oxidation, they were not effective for radiation induced oxidation.

The effort described herein seeks to improve the resistance of waste containment bags that are exposed to α radiation in an air atmosphere, which would decrease the frequency of re-packaging and consequently decrease cost (e.g. additional disposal cost of degraded bags) and worker exposure risk through controlling PE's sensitivity to air. In addition to meeting the requirement of improved α radiation resistance, the bag

must be clear, durable and flexible for handling and routine visual monitoring. This effort details the work to date for the development and testing of an α radiation resistant antioxidant for packaging material or advanced radiation resistant waste containment bag (Radbag). Three areas of study in this funding period were: (1) synthesis and characterization of nanoparticles (NPs) capable of being incorporated into PE as antioxidants for radiative environments (2) development of polymer samples containing various additives (3) test samples and evaluate activation energy of PE composites using TGA.

2.0 Experimental Procedure

2.1 Materials

Chemicals were used as received and are listed from supplier as follows. Sigma Aldrich: polyethylene (PE), iron oxide (Fe_2O_3), zinc nitrate hexahydrate, ethylene glycol, barium nitrate, and sodium hydroxide. Buckminsterfullerene were functionalized with lithium borohydride to create a C_{60}:$LiBH_4$ NP according to modified literature methods. Briefly, 10 wt.% of LiBH4 was mixed with C60 and THF in an argon glovebox. The THF was then removed under vacuum and the resultant powder was annealed at 300°C for 1 h [3, 15].

2.2 Preparation of Zinc and Doped Zinc Nanoparticles

In a typical synthesis of undoped and doped zinc oxide nanoparticles (NPs), zinc nitrate-6-hydrate ($Zn(NO_3)_2 \bullet 6\ H_2O$) is added to 32 mL of deionized water to obtain a Zn^{2+} solution. Afterwards, 4 mL of a base (1M NaOH) was added dropwise (2 min) into the zinc solution with magnetic stirring at room temperature to get a colloid system, which was maintained under stirring for 10 min. Then, the reaction mixture was transferred into a glass vessel for use in a microwave accelerated reaction system (CEM Discovery) and operated at 50 W for a period of 10 minutes. A reaction temperature threshold was set in the program to ensure that the measured reaction temperature did not exceed 100°C during the reaction.

2.3 Characterization of Synthesized Zinc and Doped Zinc Nanoparticles

The structural properties of ZnO and doped – ZnO nanoparticles were investigated by scanning electron microscopy (SEM) and Fourier Transform Infrared (FTIR) spectroscopy. The studies were carried out to determine the chemical composition, light transmission and morphology, respectively. Synthesized ZnO and doped-ZnO powders were also characterized by X-Ray diffraction with a Siemens D500 diffractometer. Diffraction patterns were recorded from 10 to 80° 2θ with a step size of 0.06° at 35 kV and 25 mA. The average crystallite size D (Table 1) of the ZnO and doped – ZnO nanostructures were calculated using Scherrer's formula (Equation 1)

$$D = \frac{0.9\lambda}{\beta cos\theta} \quad (1)$$

where λ is the X-ray wavelength of Cu-Kα radiation source, β is the full width at half maximum intensity of the diffraction peak located at 2θ and θ is the Bragg angle.

Table 2-1. Structural parameters of Ba-doped and undoped ZnO nanoparticles.

Sample	2θ Value Along (101) plane	Crystallite Size D (nm)
ZnO	36.1386	25.53
2.5% BaZn	36.2109	26.39
5.0% BaZn	36.1245	25.32

2.4 Preparation and Characterization of Polyethylene and Composite Polyethylene Films

PE films (see Figure 6-4) were made from linear low-density polyethylene (LLDPE) pellets using a lab-scale extruder, Filabot Original, with a custom-made 1/16 in. x 1 in. extruder die. PE composite films were made by adding the additives to 15 g of PE and mixing well to ensure even coating of the LLDPE pellets. The mixture was then poured into the hopper of the extruder and PE films were extruded at 190 °C. All the PE strips were then cut into 2 in. pieces and pressed using a Carver press at 2 metric tons and 266 °F for 10 min.
A PerkinElmer Pyris 1 thermogravimetric analyzer was used for TGA experiments. Decomposition profiles were obtained while heating at 2, 5, 10 and 20°C/min between 50 to 600°C for a sample size of ~15 mg.

3.0 Results and Discussion

3.1 Microwave Synthesis of Doped Zinc Nanoparticles

3.1.1 X-Ray Diffraction

The X-ray diffraction (XRD) spectra of the undoped and barium doped zinc oxide (ZnO) nanoparticles are shown in figure 3-1. All samples exhibit sharp diffraction peaks conforming to (1 0 0), (0 0 2), (1 0 1), (1 0 2) as shown in figure 3-1 while (2 0 0), (1 0 3), (1 1 0) peaks are not shown. The listed diffraction peaks are indicative of a wurtzite hexagonal ZnO structure in conformity with the database of the JCPDS number 36-1451. For neat ZnO NP, no secondary phase was detected in the XRD pattern. However, in the presence of the Ba^{2+} ion the diffractograms translocated to higher 2θ to incorporate the large radius of the Ba atom. The appearance of a secondary phase was noted with the addition of the Ba dopant, indicating an augmentation of the structure as well as incomplete incorporation of the Ba^{2+} at the concentrations tested.

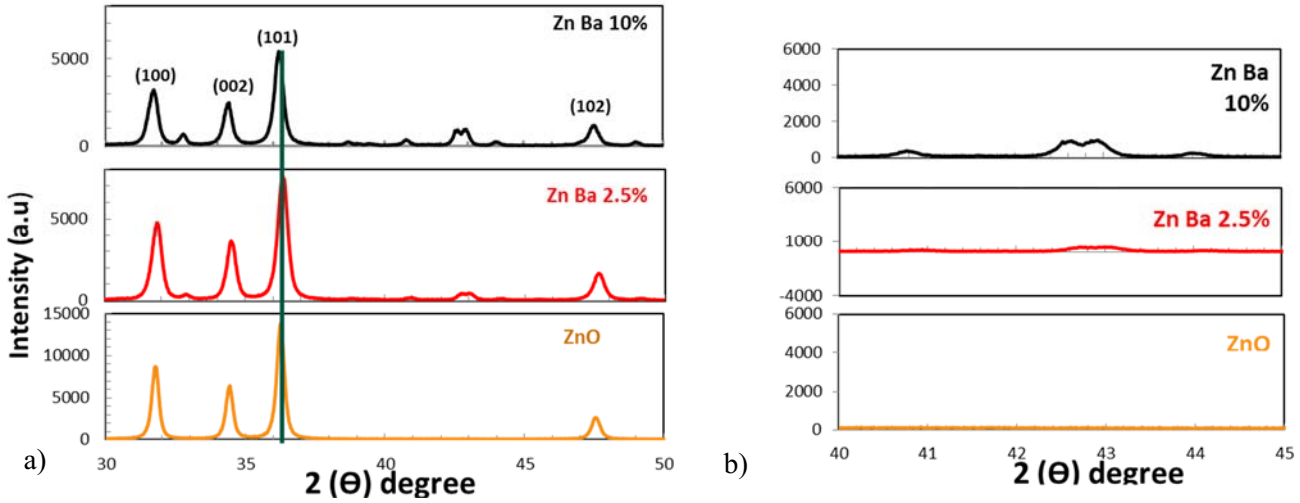

Figure 3-1. XRD patterns at (a) 2θ = 30° – 50° and (b) 2θ = 40° – 45° of Ba-doped and undoped ZnO NPs. Curve in orange indicates the undoped ZnO, red indicates zinc doped with 2.5 % barium (ZnBa 2.5%) and black indicates zinc doped with 10% barium (ZnBa 10%).

3.1.2 SEM Characterizations

The surface morphologies of the prepared samples were characterized by SEM, as depicted in figure 3-2. The SEM images showed differences in the morphology of undoped and Ba-doped ZnO NPs and nanostructural homogeneities. SEM results showed that the sintered powders were highly agglomerated, while chemical mapping identified larger concentrations of barium in agglomerated regions. Further research will be conducted to determine the impact of the higher concentrations of Barium on the physical and chemical properties of the Zinc-Barium NP.

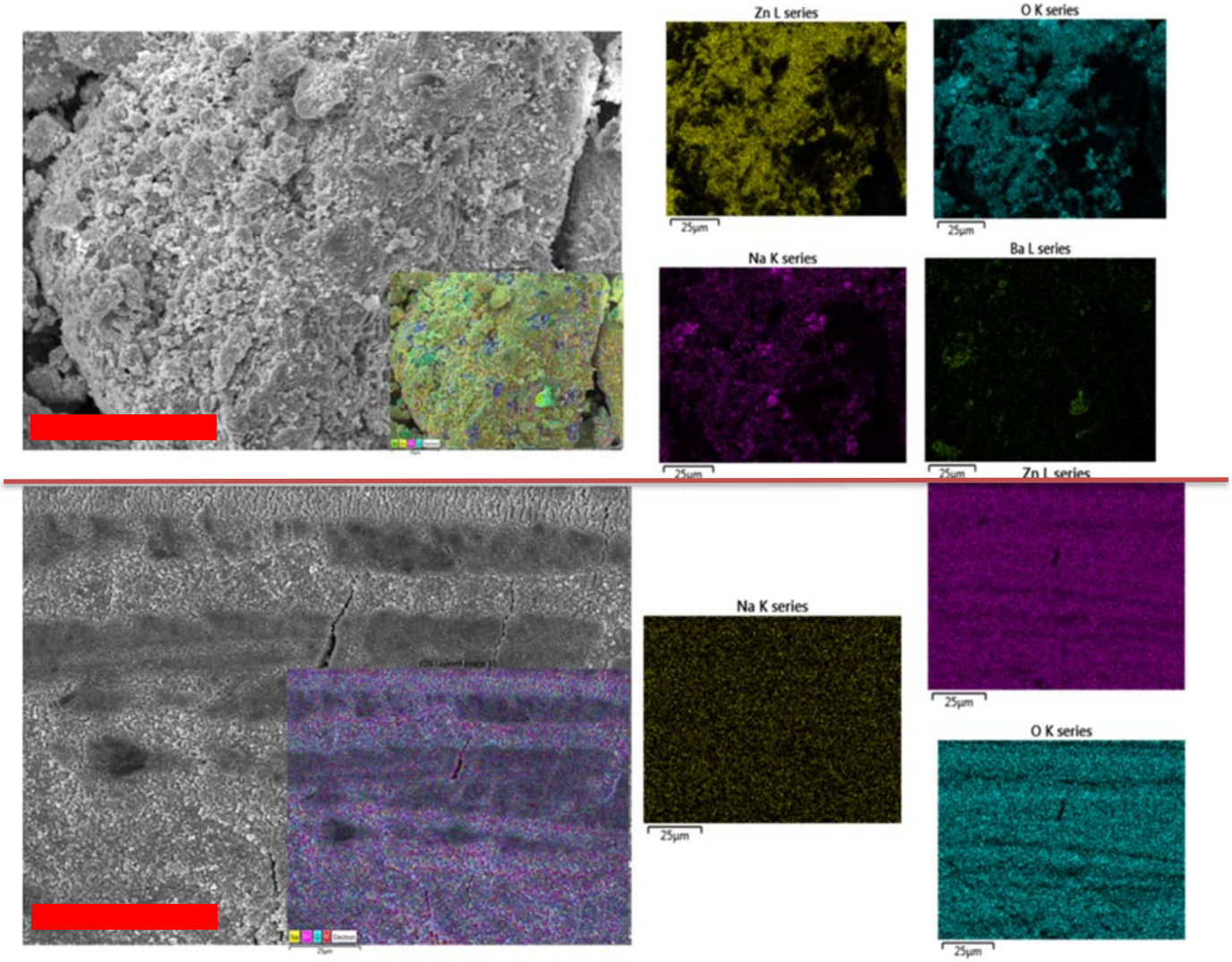

Figure 3-2. SEM images of the ZnO (bottom) and 2.5% Ba doped ZnO (top) NPs. Compositional scans show the relative dispersion of individual elements in the NP. The red scale bars in the larger SEM scans are 25 µm.

3.2 Characterization of Polyethylene and Composite Polyethylene Films

3.2.1 Impact of Air on the Degradation of PE

TGA scans of PE thermal degradation in argon and air were performed and analyzed to determine the sensitivity of PE to oxygen. The scans were taken at a rate of 10°C/min from the range of 50°C – 600°C. In both air and argon, PE degrades in a single step beginning at ~260°C and ending at ~509°C and ~523°C, respectively. The onset of the degradation is likely due to the loss of antioxidants in the system followed by loss of small molecular groups at lower temperatures. Finally, the degradation of larger molecular groups occurs at higher temperatures.

Non-isothermal methods have been used extensively for the determination of kinetic parameters. Authors have employed different computational methods among which the Freeman Carroll, Flynn-Wall-Ozawa, Coats Redfern, Horowitz Metzger, Doyle modified by Zsako, and Satava-Skvarfi methods are well known and have been tested by several researchers [12]. In this study, the Kissinger method was utilized [11]. The previous method of using activation energies (E_a) for the thermal degradation of PE in both air and argon were determined and compared.

The conversion rate (dx/dt) of a TGA's dynamic experiment at a constant heating rate of (β) is expressed as Equation 2:

$$\frac{dx}{dt} = \frac{A}{\beta} exp\left(\frac{-E_a}{RT}\right) f(x) \quad (2)$$

where: E_a is the activation energy of the process, R is the gas constant (8.314 J mol^{-1} K^{-1}), f(x) is the type of functional relation, T is the absolute temperature (K), and A is the pre-exponential factor (min^{-1}). Using this as a background, Kissinger [11, 13] developed a procedure to estimate the activation energy in physical or chemical processes from data of several non-isothermal tests conducted at constant heating rates (constant heating rates for each test; however, the rates were different between tests). Kissinger demonstrated that for a series of non-isothermal tests:

$$\frac{\beta E_a}{RT_m^2} = -qk_o exp\left(-\frac{E_a}{RT_m}\right) \quad (3)$$

Or

$$\frac{d\ln(\beta/T_m^2)}{d(1/T_m)} = -\frac{E_a}{R} \quad (4)$$

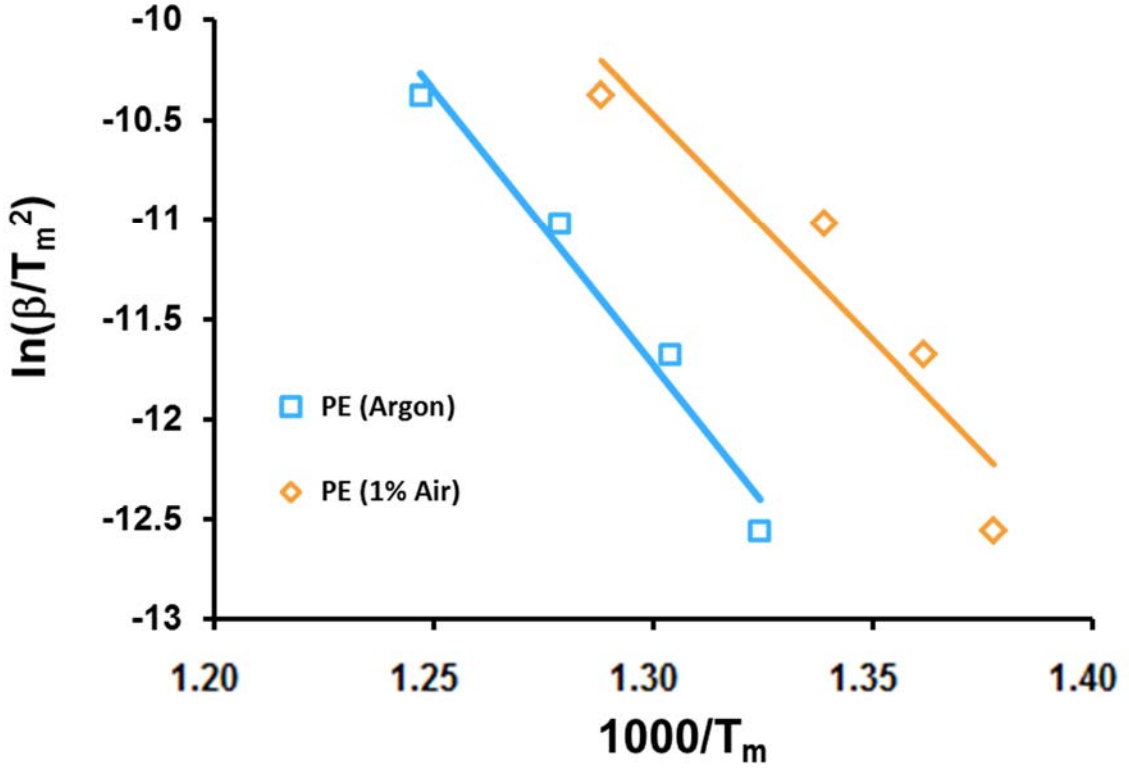

Figure 3-3. Kissinger plot obtained by TGA data at different heating rates for PE in an Argon atmosphere (□) and PE in an atmosphere of 1% air (◊).

In equation 4, β is the rate of heating during testing, T_m is the maximum temperature derived from the DTA curve, R is the gas constant and E_a is the activation energy. According to equation 4, a plot of $\ln(\beta/T_m^2)$ versus $1/T_m$ leads to a straight line with the slope equal to $-E_a/R$.

Figure 3-3 shows the Kissinger plot for four heating rates of PE in both argon and 1% air atmospheres. PE is calculated to have activation energy of ~229.28 kJ mol^{-1} in an argon atmosphere; however, the slope of PE in the air atmosphere is lower and shifted to the right when compared to the slope of PE in an argon environment. Subsequently, the activation energy of PE calculated for the degradation in ~1% air and was found to be ~187.81 kJ mol^{-1}. The value of the E_a in 1% air is significantly higher than previously reported values for the E_a in pure air which was ~53 kJ mol^{-1} [14]. The decrease in the E_a illustrates the impact of oxygen on the degradation of PE and highlights the need to find a system that will mitigate the level or potency of oxygen in PE.

3.2.2 Evaluation of Composite PE Films

Composite PE films were created by a combination of PE and NPs. Prepared films were tested using TGA. Initial studies of the activation energy of PE and composite PE began with the evaluation of two composite systems that were previously evaluated by this group. The Kissinger equation was used to calculate the activation energies of the PE and PE composite systems. Figure 3-4 shows the Kissinger plots for the tested systems. PE maintains an activation energy of ~229.28 kJ mol^{-1} in an argon atmosphere; however, the incorporation of Buckminster fullerene: lithium borohydride (C_{60}:$LiBH_4$) to the PE composite did not change the value of E_a (~229.43 kJ mol^{-1}) that is within statistical error. Since TGA testing of C_{60}:$LiBH_4$ was conducted in an inert atmosphere, the likelihood of oxidation being the primary degradation mechanism

is low. However, it is believed that the desorption to hydrogen from the surface of the C_{60}:$LiBH_4$ [15] can interact with radicals evolved during thermal degradation, thereby providing a slight increase to the activation energy of the PE:C_{60}:$LiBH_4$ composite. The activation curves for both PE and the PE:C_{60}:$LiBH_4$ composite are similar. However, the activation energy curve for the incorporation of iron oxide into the PE matrix shows a much different behavior. With the incorporation of Fe_2O_3, a shift in the Kissinger line as well as a decrease in the slope are noted. The decrease in the E_a, calculated from the decreased slope is indicative of a reduction in the energy required to begin to the degradation process in PE. Ultimately, the decrease in the activation energy from PE (~229.28 kJ mol^{-1}) to the PE composite containing iron (~181.36 kJ mol^{-1}) is attributed to thermal and oxidative degradation catalyzed by both the thermal transfer from iron to the PE matrix and the oxidative degradation at the iron - polymer interface. [15, 16]

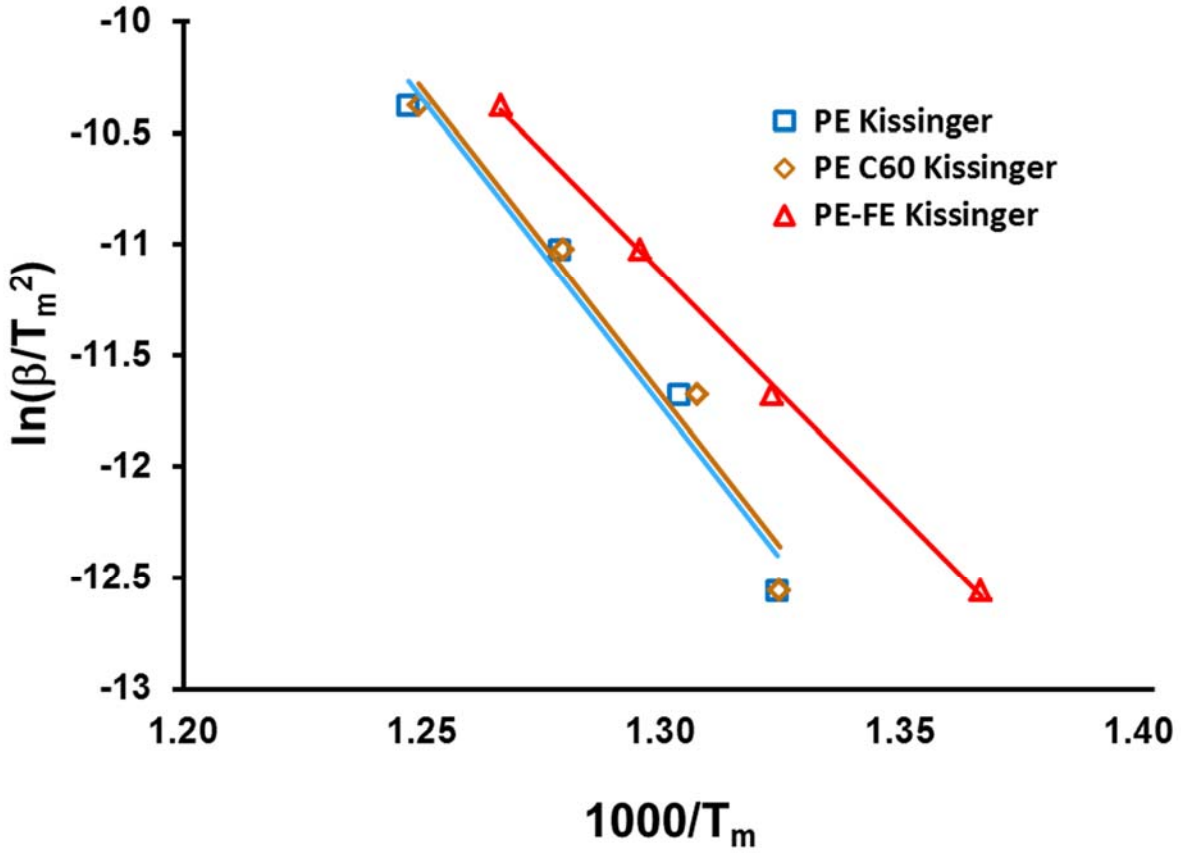

Figure 3-4. TGA data at different heating rates for PE (□), a composite of PE and C_{60}-Lithium Borohydride (LiBH) (◊) and a composite of PE and iron oxide (Δ) in an Argon atmosphere.

Mass loss from TGA of PE and four PE composites at a heating rate of 10°C min^{-1} under 1% air atmosphere are shown in figure 3-5. Doped and undoped composites show a single degradation phase; however, PE with zinc incorporated shows a slow catalytic degradation that begins at ~200°C and results in a 5% mass loss before a noticeable loss is noted in PE or other composites samples. To mitigate the impact of catalytic loss of zinc, a blend of zinc and silica is made into a composite blend with PE and showed improvements in the thermal stability of the zinc based composite at levels that are comparable to the Aglion® (hybrid Si blend). Both the PE:Agl and PE:BaZn composites at 1.5 mmol are comparable to the PE degradation curve. For all tested samples, the PE:BaZn composite has a higher curve than the PE and displayed better thermal stability over a wide range of temperatures than other samples.

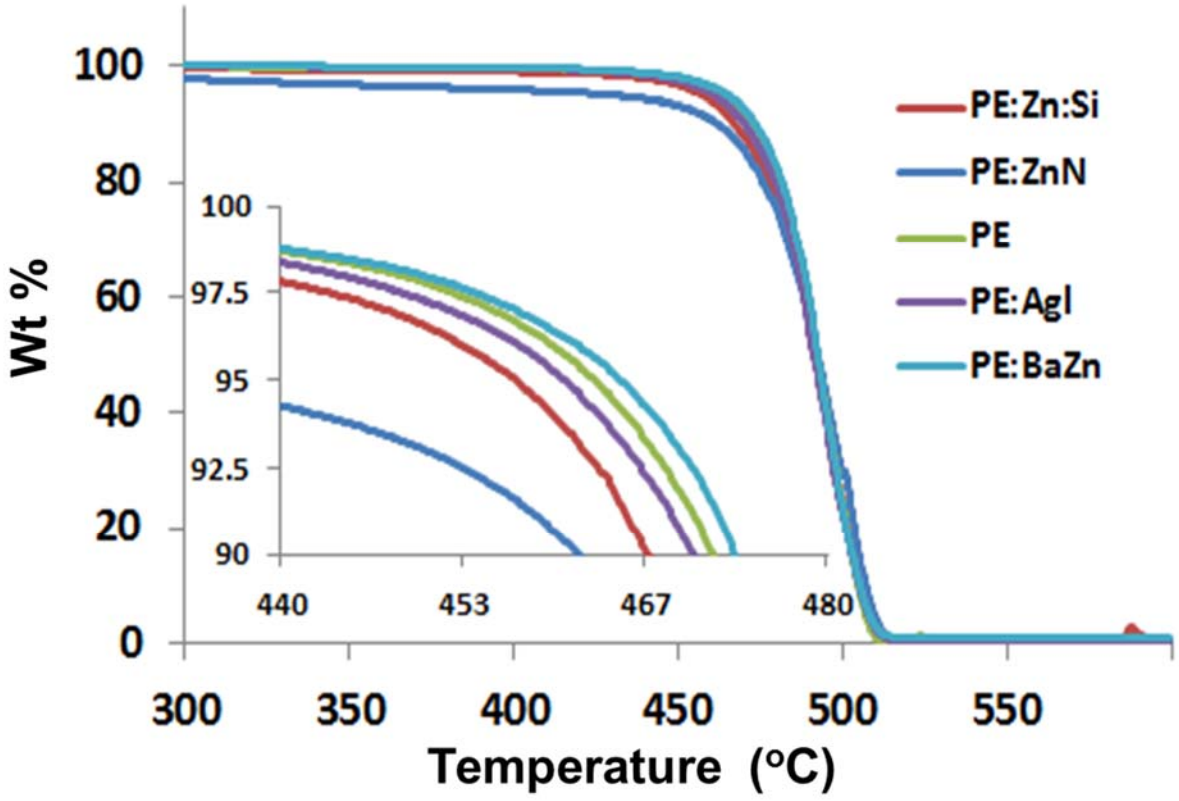

Figure 3-5. TGA curves for the thermal decomposition of PE (black line) and as a composite with ZnO (red line), ZnO:Si (tan line), AgI (blue line), and BaZn (green) in air at 10°C/min

The thermal profile of prepared films was tested using TGA. Activation energy of PE, in both argon and ~1% air, was compared between PE:AgI and PE:BaZn composites, which showed statistical differences from PE in ~1% air during thermal degradation. Kissinger equation was used to calculate the activation energies of the PE and PE composite systems. Figure 3-6 shows the Kissinger plots for the tested systems. PE's maintains activation energy of ~229.28 kJ mol^{-1} in an argon atmosphere; while the PE in air showed activation energy of 187.81 kJ mol^{-1}. This is > 20% decrease in the activation energy. Calculated E_a for the 1.5 mmol of PE:AgI and PE:BaZn composites, in an air environment, were 186.23 kJ mol^{-1} and 202.94 kJ mol^{-1}, respectively. This increase in activation energy approaches the activation energy of pristine PE and suggests the addition of these additives could mitigate thermal degradation of PE composites.

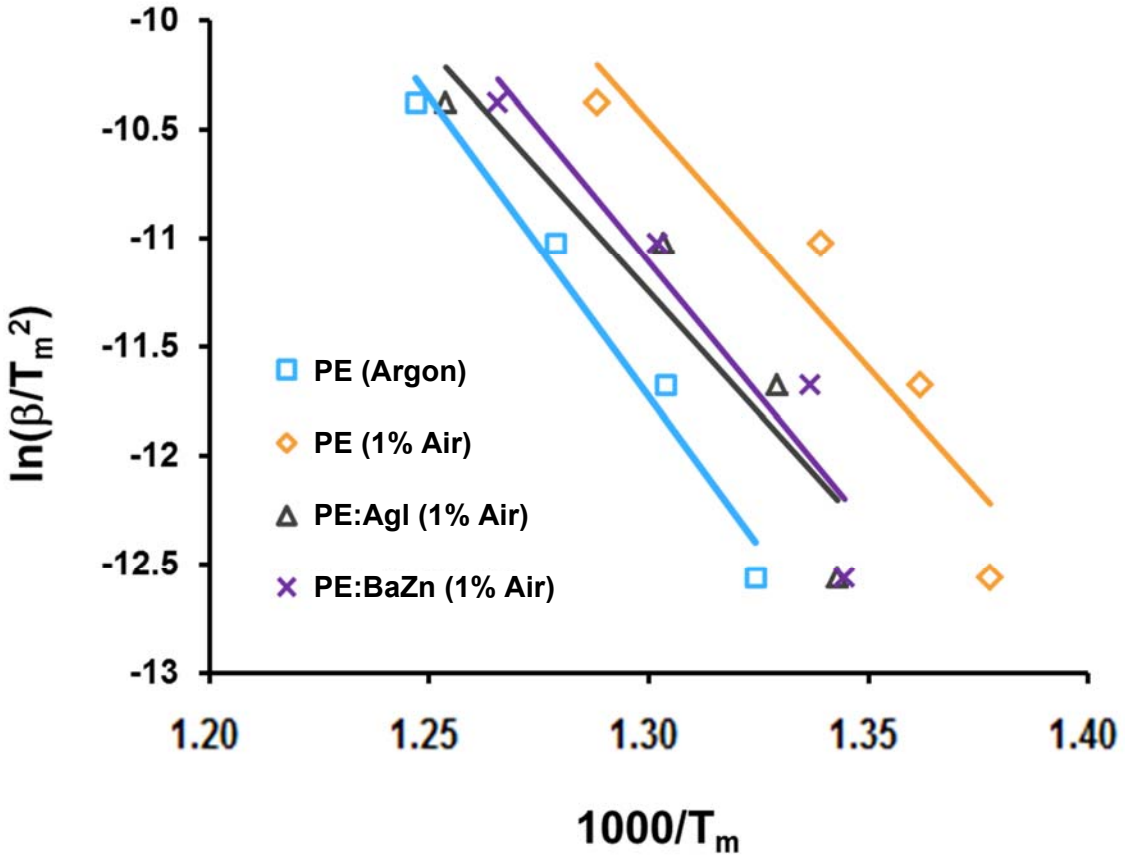

Figure 3-6. Kissinger plot obtained by TGA data at different heating rates for PE in an Argon atmosphere (□) as well as PE (◊), polyethylene barium doped zinc composite (X - PE:BaZn) and polyethylene Agilon® (Δ- PE:Agl)composite in an atmosphere of 1% air.

4.0 Conclusions

Oxygen, which is a component of atmospheric air, is an essential contributor to the thermal and radiolytic degradation of plastics. This effort evaluated the sensitivity of undoped and doped PE to air using thermogravimetric analysis (TGA). The activation energy of undoped PE in air and an inert argon environment consistently show a ~3% difference in the maximum differential thermal analysis curve. Nanoparticle doping can be used to influence the activation energy of PE in both inert and air atmosphere as evidence by both the increase and decreasing rates of thermal degradation during this study. Both zinc oxide and iron were found to behave as catalysts for the degradation of PE as determined by the significant increase the degradation rates. Fillers capable of undergoing an Oxygen Reduction Reaction (ORR) through the liberation of a molecular hydrogen or energetic reduction of oxygen appear to have a large influence on the activation energy of PE. Barium doped zinc oxide as well as C_{60} undergo ORRs and show improved properties when compared to pristine PE.

5.0 Recommendations, Path Forward or Future Work

5.1.1 Recommendations

Work to further elucidate the impact of oxygen reduction, specifically the reduction of oxygen activated by the presence of a radiolytic source should continue. To achieve the highest rate of return for this endeavor, a partnership with a compounding company or a university that is capable of create PE composite samples with a high degree of particle dispersion in the PE matrix is imperative. The simplest next step is to find a compounder and begin the evaluation of higher percentages of NP in the composite.

5.1.2 Path Forward and Future Work

The use of antioxidants to delay the onset of degradation in polymers is a mature study; however, investigations to synthesize antioxidant for radioactive environments have not been the focus of studies because there is little industrial value to create such a product and little-to-no industrial capabilities to test these products. This effort is the first known to date that has evaluated a pathway to trap and/or mitigate oxygen in a polymer using external mechanisms that is excited by the energy of an α particle. To accelerate work, this could be extended to several polymer systems that are currently in use in nuclear environments including fittings, valves, lubricants and fixatives. Additional funding and partnerships will be required to further investigate. We have begun the process to find partners with a vested interest in this technology and may soon begin the mutual develop of technologies capable of behaving as antioxidants at high temperature and in radiolytic environments.

The impact of oxygen reduction in plastics will be essential to the on-going success of the radiation proof plastics program. Insight gained through a combination of modeling and hands-on-research will help to create a wealth of information is an area that has not yet been explored. This endeavor is ideally suited for cross-functional in-house researchers as the Basic Energy Sciences program has laid the ground work for developing and modeling the impact of oxygen reduction catalyst in several systems. Future research will look to leverage this competency as we explore the ability to further understand and expand the technology developed into adjacent arenas.

6.0 References

[1] Dauphin, J. "Radiation Effects in Materials" *Rad. Phys. and Chem.*. **1994**, 43, 47-56.

[2] Onishi, Y., Shiga, T., Ohkawa, Y., Katoh, H., Nagasawa, K., Okada, T., Saimen, K., Itano, F., Murano, Y., Tsujita, Y., Yagi, T., Morita, Y., Seguchi, T., "Study on Polymer Materials for Development of the Super 100 MGy-Radiation Resistant Motor". *Polym. J.* **2004**, 36, 617-622.

[3] Christian, J.H., Teprovich, Jr, J.A., Wilson, J., Nicholson, J.C., Truong, T.T., Kesterson, M.R., Velten, J.A., Wiedenhover, I., Baby, L.T., Anastasiou, M., Rijal, N., Washington, II, A.L., "Developing Radiation Tolerant Polymer Nanocomposites Using C_{60} as an Additive. *RSC Adv.* **2016**, 6, 40785-40792.

[4] Singh, A., "Irradiation of Polyethylene: Some Aspects of Crosslinking and Oxidative Degradation" *Radiation Physics and Chemistry*, 1999, 56, 375-380

[5] Gillen K.T., Clough, R.L., Jones, L.H. "Investigation of Cable Deterioration in the Containment Building of the Savannah River Nuclear Reactor", *Prepared for U.S. Nuclear Regulatory Commission*, NUREG/CR-2877, SAND81-2613, 1982

[6] Reed, D.T., Hoh, J., Emery, J. Hobbs. D., "Radiolytic Gas Production in the Alpha Particle Degradation of Plastics" *Waste Management Symposia*, 1992, 2, 1081-1085.

[7] Peterson, J.D., Vyazovkin, S., Wight, C.A., "Kinetics of the Thermal and Thermo-Oxidative Degradation of Polystyrene, Polyethylene and Poly(Propylene)", *Macromol. Chem. Phys*., **2001**, 202, 775-784.

[8] Vasconselos, G. da C., Mazur, R.L., Ribeiro, B., Botelho, E.C., Costa, M.L., "Evaluation of Decomposition Kinetics of Poly (Ether-Ether-Ketone) by Thermogravemetric Analysis" *Mat. Res.*, **2014**, 17, 227-235.

[9] Suenaga, T., Noguchi, K., Okamoto, Y., Sekii, Y., Miyake, K., "Effects of Antioxidents on Thermal Degradation of EPDM and XLPE." *Proceedings of 2008 International Conference on Condition Monitoring and Diagnosis, CMD 2008,* **2007**, 294-298

[10] Seguchi, T., Tamura, K., Oshima, T., Shimada, A., Kudoh, H., "Degradation Mechanisms of Cable Insulation Materials During Radiation-Thermal Ageing in Radiation Environments," *Rad. Phys, Chem.*, **2011**, 80, 268-273.

[11] Kissinger, H.E.,"Reaction Kinetics in Differential Thermal Analysis," *Anal. Chem*., **1957**, 29, 1702-1706.

[12] Wahab, MMM, "Thermal Decomposition Kinetics of Some New Unsaturated Polyesters," *Thermochimica Acta*, **1995**, 256, 271-280.

[13] Kissinger, H.E., "Variation of Peak Temperature with Heating Rate in Differential Thermal Analysis," *J. Res. NBS*, **1956**, 217-221.

[14] Vasile, C., Costea, E., Odochain, L., "Thermooxidative Decomposition of Low Density Polyethylene in Non-Isothermal Conditions," *Thermochimica Acta*, **1991**, 184, 305 – 311.

[15] Ward, P.A., Teprovich, J.A., Peters, B., Wheeler, J., Compton, R.N., Zidan, R., "Reversible Hydrogen Storage in a $LiBH_4$-C_{60}Nanocomposite," *J. Phys. Chem. C*, **2013**, 117, 22569-22575.

[16] Gonzalez-Bahamon, L.F., Mazille, F., Benitez, L.N., Pulgarin, C, "Photo-Fenton Degradation of Resorcinol Mediated by Catalysts Based on Iron Species Supported on Polymers," *J. Photochemistry and Photobiology A: Chemistry*, **2011**, 217, 201-206.

[17] Haham, H., Grinblat, J., Sougrati, M-F., Stievano, L., Margel, S., "Engineering of Iron-Based Magnetic Activated Carbon Fabrics for Environmental Remediation," *Materials*, **2015**, 8, 4593 – 4607.

[18] Zazoum, B. David, E., Ngo, A.D., "Correlation Between Structure and Dielectric Breakdown in LDPE/HDPE/Clay Nanocomposites," *ISRN Nanomaterials*, **2014**, 2014, 1-9.

Appendix A.

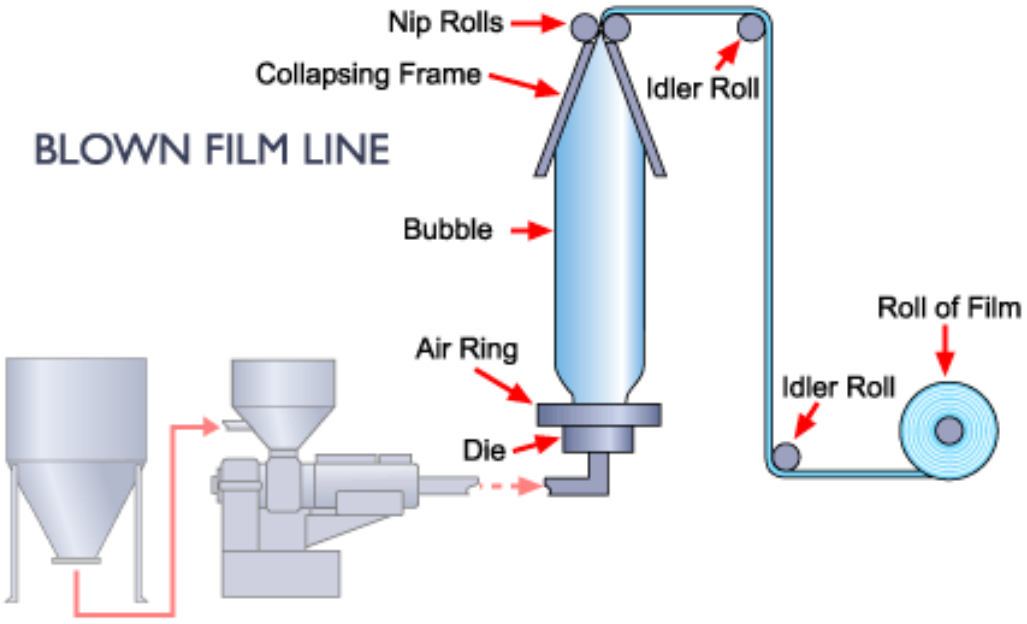

Supplemental Figure 1. Schematic of a polyethylene blown film extrusion line, typically used to create polyethylene bags.

Plastics extrusion is a high-volume manufacturing process in which raw plastic is melted and formed into a continuous profile. Extrusion produces items such as pipe/tubing, weather stripping, fencing, deck railings, window frames, plastic films and sheeting, thermoplastic coatings, and wire insulation. This process starts by feeding plastic material (pellets, granules, flakes or powders) from a hopper into the barrel of the extruder. The material is gradually melted by the mechanical energy generated by turning screws and by heaters arranged along the barrel. The molten polymer is then forced into a die, which shapes the polymer into a pipe that hardens during cooling. Blown film co-extrusion lines are designed to produce high performance barrier, printing and laminating films in an efficient and cost-effective manner.

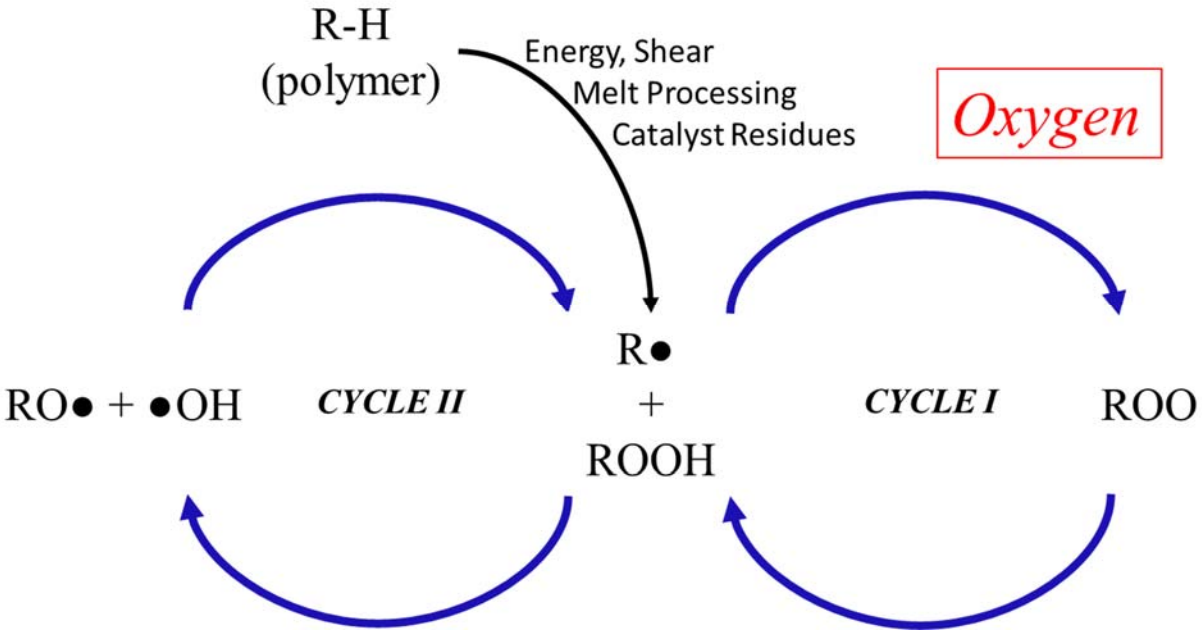

Supplemental Figure 2. Reaction schematic of the degradation pathway for polymers. Note the reaction pathway is similar for many reactions including; energetic systems (radiation), shearing, melt processing and catalytic.

Polymer degradation is a change in the properties (tensile strength, color, shape, etc.) of a polymer or polymer-based product under the influence of one or more environmental factors such as heat, light or chemicals such as acids, alkalis and some salts. These changes are usually undesirable, such as cracking and chemical disintegration of products, except for cases of deliberately lowering the molecular weight of a polymer for recycling. Biodegradation has been used in this arena. The changes in properties are often termed "aging". Figure 6-2, shows a generalized schematic of a degradation process that is relevant to several high-volume commodity thermoplastics including PE. Polymers are susceptible to atmospheric attack by oxygen, especially at elevated temperatures [7-10, 12, 14] and under high loading of energy (electricity, radiation) similar behaviors are noted to exist [18]. Polyethylene has a relatively simple spectrum with few peaks at the carbonyl position. Oxidation tends to start at tertiary carbon atoms because the free radicals formed here are more stable and longer lasting, making them more susceptible to attack by oxygen. The carbonyl group can be further oxidized to break the chain, this weakens the material by lowering its molecular weight, and cracks start to grow in the regions affected.

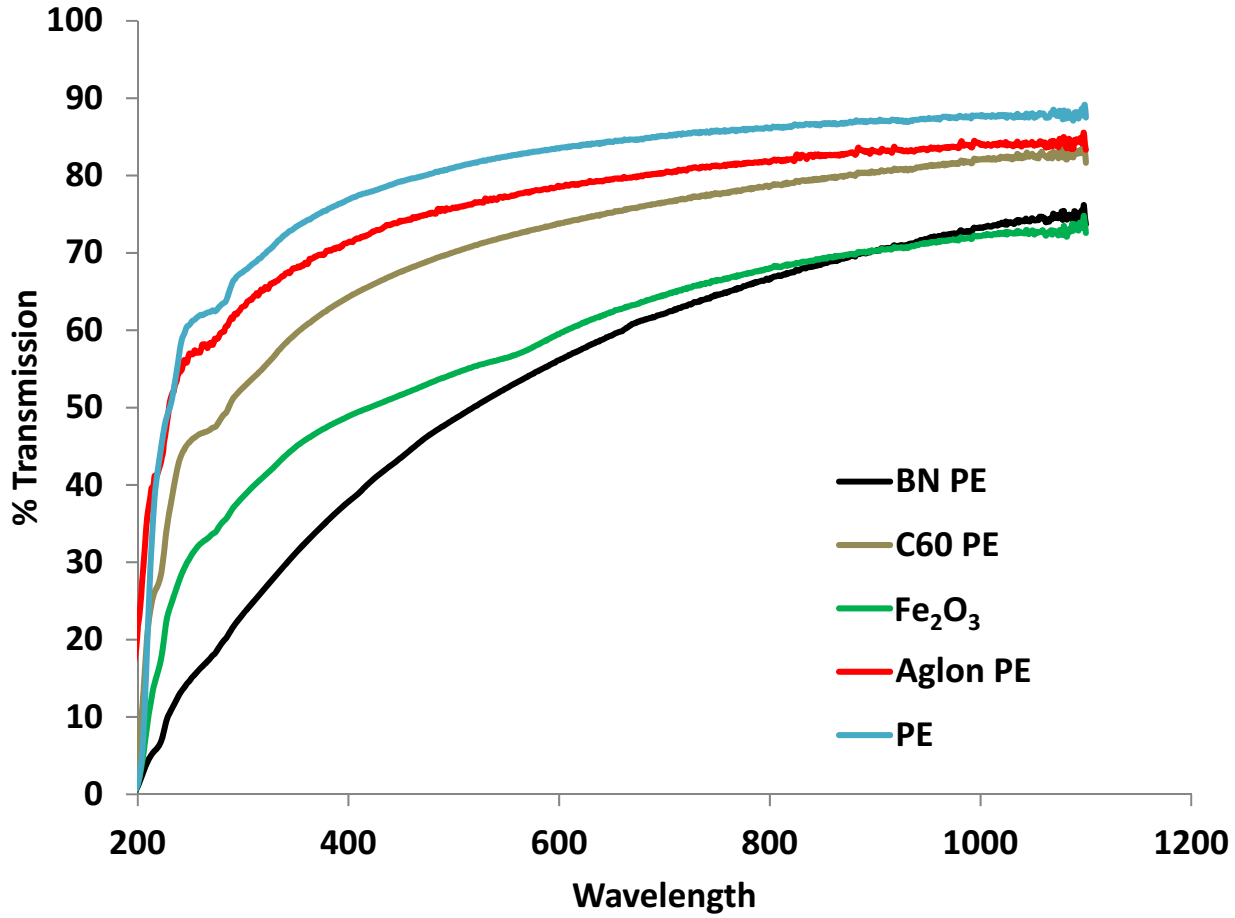

Supplemental Figure 3. UV-Vis Spectra of the (doped) PE films at a thickness of ~85 ± 5 µm.

UV-Vis refers to absorption spectroscopy or reflectance spectroscopy in the ultraviolet-visible spectral region. The absorption or reflectance in the visible range directly affects the perceived color of the chemicals involved, due to atoms and molecules undergoing electronic transitions. In this study understanding how the composite material absorbed light and the subsequent transitions that were the result of that absorption was used as a screening tool for the optical clarity of the PE and PE doped films. Figure 6-3, shows that the addition of Aglon® has the lowest impact on the transmission of light with C_{60} being the next material with a low impact of the transmission. Although Fe_3O_4 has a significant impact of the transmission this material was still optically clear. This may suggest that Fe_2O_3 may possess a high degree of activity with very little energy since UV-Vis is a good indicator of electronic transitions. The inclusion of BN in to the PE matrix, creates a material that not only has a low transmission in the 200 to 700 nm range, but also is not optically clear. This combination may help to find reasonable screening tools to predict which materials to incorporate into the PE matrix that would have little impact on the optical clarity and would not be as energetic in the PE matrix.

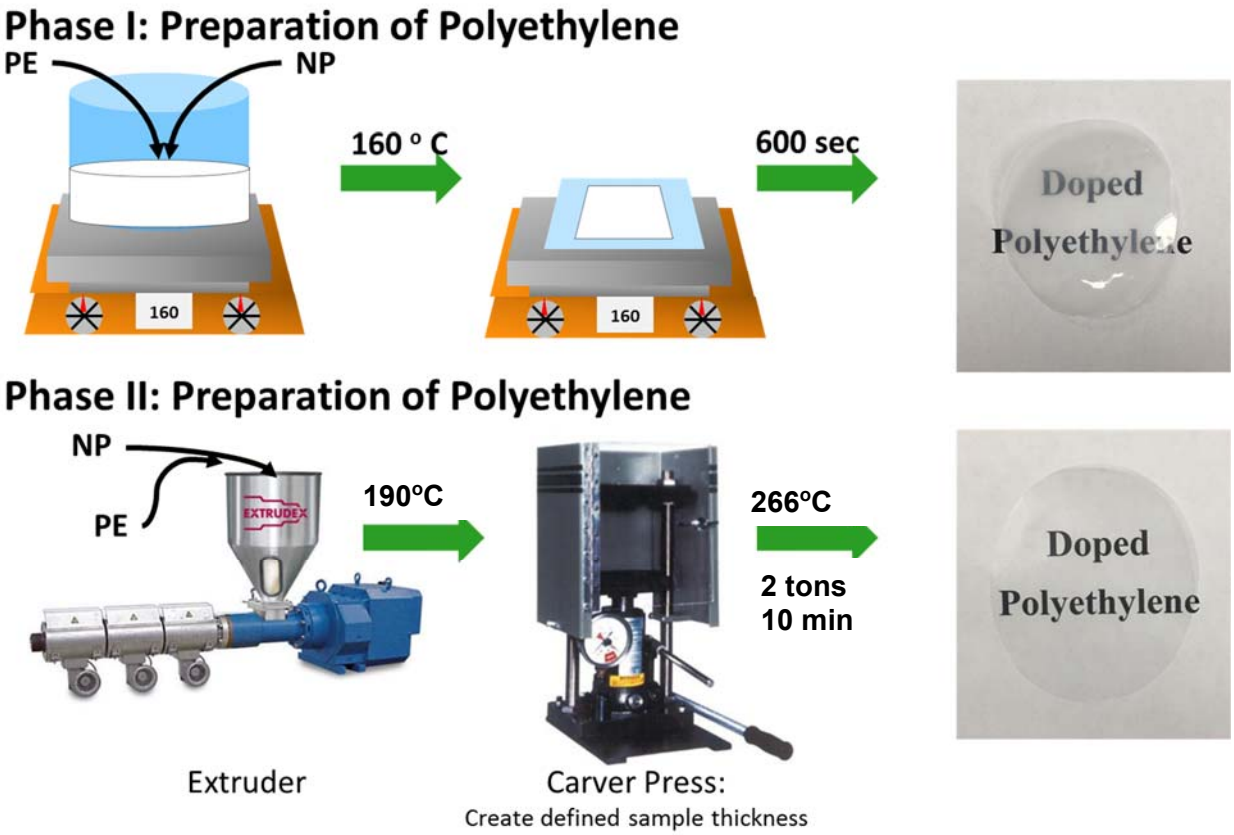

Supplemental Figure 4. Schematic of the preparation of doped PE using a modified hot plate method to produce doped PE files (Phase I) and a pilot scale process to dope PE.

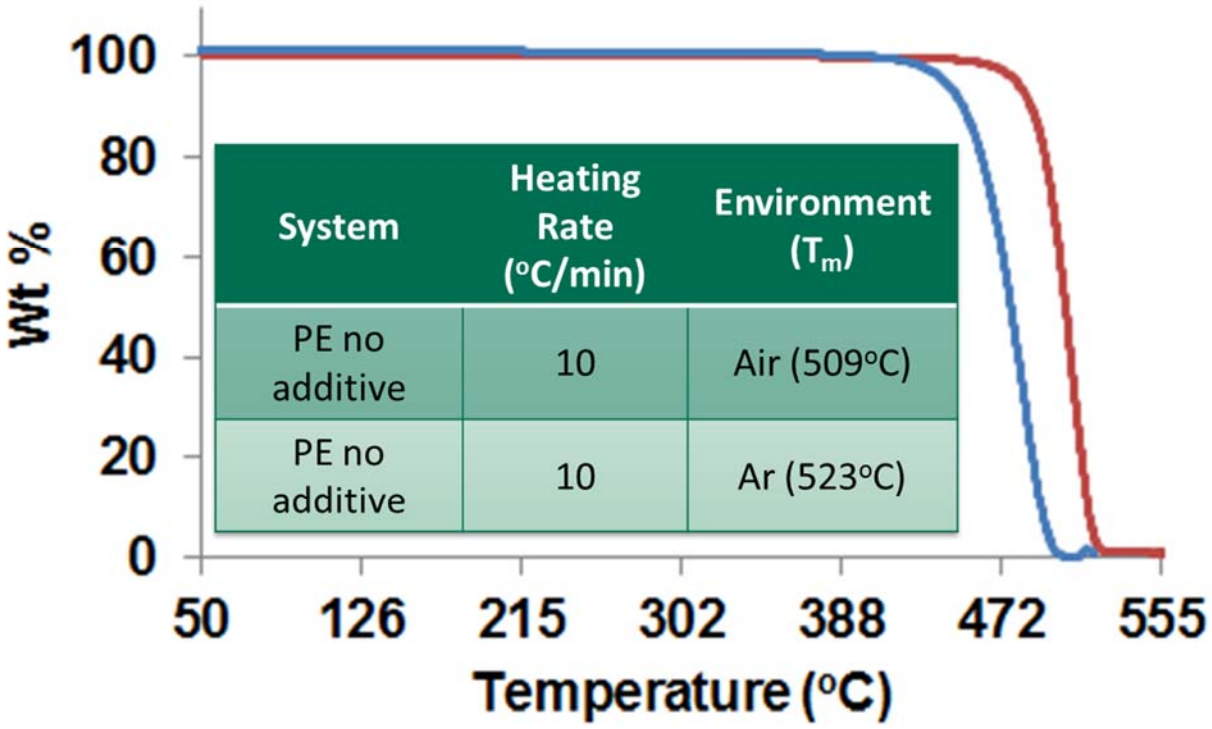

Supplemental Figure 5. Degradation of PE at 10° C/min in air (blue line) and under an argon atmosphere (red line).

Distribution:

T. B. Brown, 773-A
M. E. Cercy, 773-42A
D. A. Crowley, 773-43A
A. D. Cozzi, 999-W
D. E. Dooley, 773-A
A. P. Fellinger. 773-42A
S. D. Fink, 773-A
N. V. Halverson, 773-42A
C. C. Herman, 773-A
E. N. Hoffman, 999-W
B. B. Looney, 773-42A
J. J. Mayer, 999-W
G. A. Morgan, 999-W
F. M. Pennebaker, 773-A
L. T. Reid, 773-A
G. N. Smoland, 773-42A
B. J. Wiedenman, 773-42A
W. R. Wilmarth, 773-A
Records Administration (EDWS)
Leroy Magwood 999-2W
Jonathan Christian, 999-2W
Aaron L. Washington, II, 773-42A
Thanh-Tam Truong, 773-41A